ELSEVIER

Surface Science 505 (2002) 1–13

SURFACE SCIENCE

www.elsevier.com/locate/susc

Scanning tunneling microscopy of reconstructions on the $SrTiO_3(001)$ surface

Martin R. Castell

Department of Materials, University of Oxford, Parks Road, Oxford OX1 3PH, UK

Received 22 October 2001; accepted for publication 18 January 2002

Abstract

Scanning tunneling microscopy (STM) was used to investigate the (0 0 1) surface atomic structure of Nb-doped $SrTiO_3$ single crystals which were annealed in ultra high vacuum. Atomic resolution images of the (2×1), $c(4 \times 4)$, and $c(4 \times 2)$ reconstructions are presented. Surface structure models are proposed based on qualitative interpretation of the STM images. Surface terminations with different Ti to O ratios are considered.

Keywords: Scanning tunneling microscopy; Surface relaxation and reconstruction; Alkaline earth metals; Titanium; Surface structure, morphology, roughness, and topography; Low index single crystal surfaces; Surface defects

1. Introduction

The main interest in $SrTiO_3$ surfaces has emerged from its extensive use as a substrate for the growth of high T_c superconducting thin films. More recently it has also been investigated as a candidate for a crystalline gate dielectric in silicon-based devices [1,2], and a buffer material for the growth of GaAs on Si [3]. But in spite of the technological and scientific importance of $SrTiO_3$, the atomic structure of the crystal surfaces and their reconstructions are only poorly understood. In this paper results are presented from scanning tunneling microscopy (STM) experiments on three $SrTiO_3(001)$ reconstructions that are created through ultra high vacuum (UHV) annealing with or without argon ion sputtering. The STM images, in conjunction with published data, allow atomic surface structure models to be proposed.

1.1. $SrTiO_3$ crystal structure

$SrTiO_3$ crystallizes into the cubic perovskite structure with a 0.3905 nm lattice parameter and formal ionic charges of Sr^{2+}, Ti^{4+}, and O^{2-}. The unit cell is shown in Fig. 1a with Ti ions at the cube corners, a Sr ion in the centre of the cube, and O ions on the cube edges. The crystal viewed in the $\langle 001 \rangle$ directions is made up from a stack of alternating TiO_2 and SrO layers, so that two charge neutral (0 0 1) bulk terminations of this crystal are possible: the SrO surface, and the TiO_2 surface, as shown in Fig. 1a. The relative stability of these two surfaces has been calculated as a function of the

E-mail address: martin.castell@materials.ox.ac.uk (M.R. Castell).

0039-6028/02/$ - see front matter
PII: S0039-6028(02)01393-6

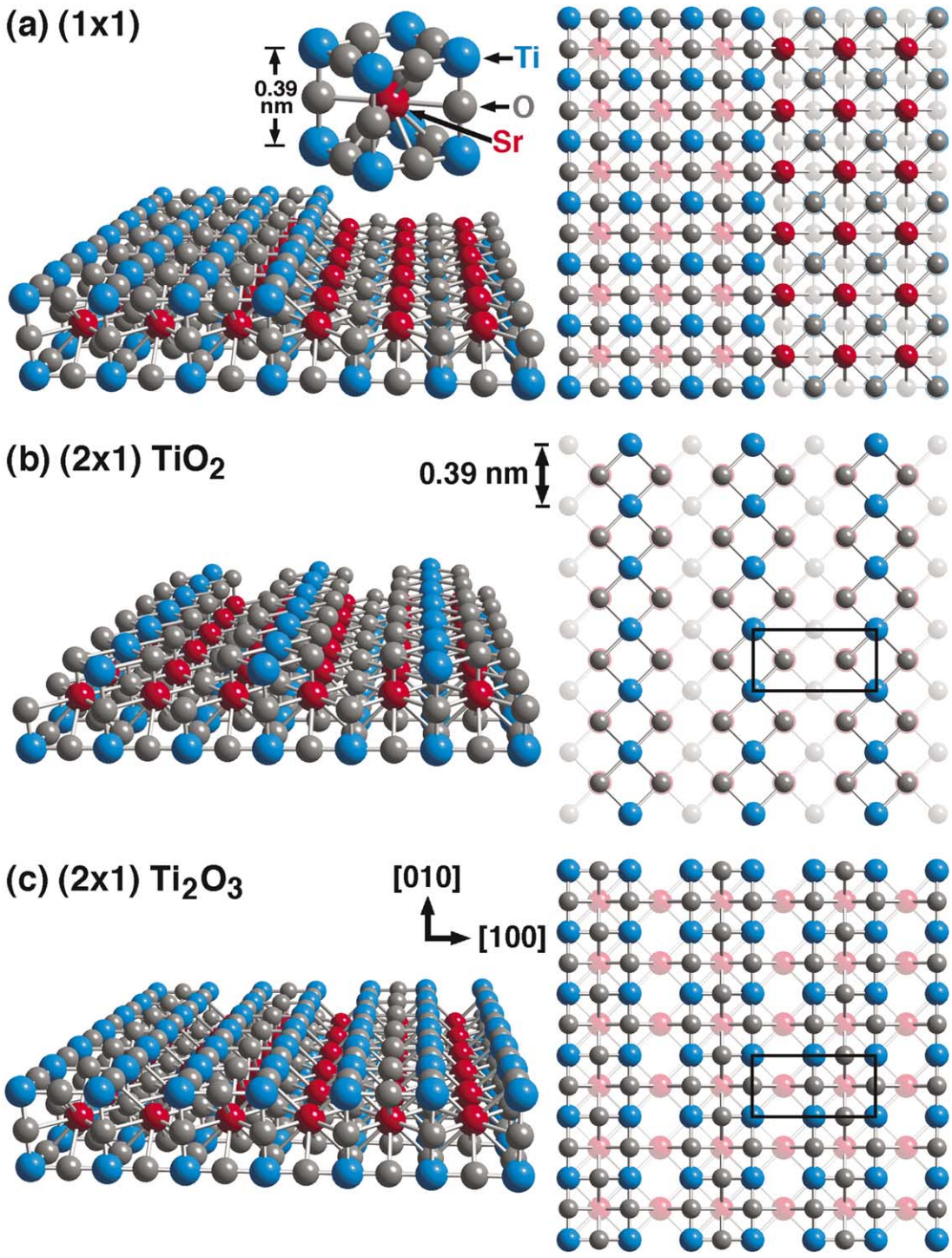
(a) (1x1)
0.39 nm
Ti
O
Sr
(b) (2x1) TiO2
0.39 nm
(c) (2x1) Ti2O3
[010]
[100]

Fig. 1. (a) The cubic unit cell of $SrTiO_3$ is shown at the top of the figure. The Ti ions (blue) are located at the cube corners, a Sr ion (red) is in the centre of the cube, and O ions (grey) are on the cube edges. A (0 0 1) surface with the two possible (1 × 1) terminations (TiO_2 on left, SrO on right) is shown in oblique view (left panel) and in top view (right panel). (b) Proposed structure of the (2 × 1) reconstructed surface with TiO_2 stoichiometry. (c) Proposed structure of the (2 × 1) reconstructed surface with Ti_2O_3 stoichiometry. In (b) and (c) the (2 × 1) unit cell is shown in the top view panels. In all top view panels the atomic layer below the surface is shown with reduced depth of colour.

chemical potential of the TiO_2 and SrO terminations [4,5]. The results show that both surfaces have comparable thermodynamic stability, so that one might expect a (0 0 1) surface of a crystal to display both types of termination.

1.2. $SrTiO_3$ electronic structure

In its stoichiometric form $SrTiO_3$ is a good insulator with a 3.2 eV band gap. The top of the valence band is dominated by O 2p states, and the bottom of the conduction band is due mainly to Ti 3d states [6–9]. n-type behaviour can be achieved through substitutional doping with La^{3+} or Y^{3+} on a Sr site, or Nb^{5+} on a Ti site, or through the introduction of bulk O vacancies by UHV annealing. p-type crystals have been created through doping with Sc^{3+} on a Ti site [10]. These doped or heavily reduced crystals are sufficiently electrically conducting to allow successful STM imaging and other surface science experiments that are sensitive to charging.

1.3. Surface structure studies on $SrTiO_3$(0 0 1)

Previous studies on $SrTiO_3$(0 0 1) have produced a multitude of data depending on the preparation of the surface. To date the reported reconstructions of the (0 0 1) surface are: (1 × 1), (2 × 1), (2 × 2), c(4 × 2), $(\sqrt{5} \times \sqrt{5})R26.6°$, and c(6 × 2). In this paper an additional structure is presented, the c(4 × 4) reconstruction, and in a future publication the (6 × 2) reconstruction will be shown [11].

The most widely studied $SrTiO_3$(0 0 1) surface is the (1 × 1) termination. Cleavage of $SrTiO_3$ crystals in UHV has been used to prepare what is presumably a two termination surface as shown in Fig. 1a, but because $SrTiO_3$ does not cleave well this process results in only weak (1 × 1) low energy electron diffraction (LEED) patterns [6]. Polished and annealed samples show (1 × 1) surface order, although it appears that annealing in an O_2 environment is necessary to prevent O deficient surface phases from forming [12–15]. The SrO termination of the two termination (1 × 1) surface can be removed through a chemical etch. Ion scattering spectroscopy showed that with the use of this etch it is possible to create substrates that are only TiO_2 terminated [12,16,17].

Atomic force microscopy and STM have been used to measure step heights between atomically flat terraces. A half unit cell height step (0.2 nm) would indicate that both TiO_2 and SrO terminations are present. Most of these studies show only unit cell high steps [18–24], although under certain specimen preparation conditions half unit cell height steps were also observed [25–27].

Annealing $SrTiO_3$(0 0 1) in a UHV environment has been investigated through electron diffraction and reported to give rise to (2 × 2) order [13,15, 28] or two domain (2 × 1) order [23,25,29]. An early report [30] of STM images of the (2 × 2) reconstruction were incorrectly interpreted, and later discovered to be images of the $(\sqrt{5} \times \sqrt{5})$-$R26.6°$ reconstruction [19,31–33]. Annealing in an H_2 environment has been reported [25] to give rise to the c(4 × 2) reconstruction, whereas annealing in O_2 causes c(6 × 2) ordering [24,25, 29].

While there is clearly extensive experimental data of the $SrTiO_3$(0 0 1) reconstructions, the interpretation of these results has been complicated by a number of factors including non-stoichiometry of the surface layer, the possibility of simultaneously having TiO_2 and SrO crystal terminations present, and the effect of surface segregation of impurities. Most reconstructions have been attributed to ordering of oxygen defects.

However, no detailed atomic structure models exist, apart from the recently proposed Sr adatom model of the $(\sqrt{5} \times \sqrt{5})R26.6°$ reconstruction [33]. In the work presented here atomic structure models of three reconstructions are proposed through interpretation of high resolution STM images.

2. Experimental method

Nb-doped $SrTiO_3$ single crystals with epi-polished (0 0 1) surfaces were supplied by PI-KEM, Surrey, UK. The 0.5% molar Nb content was determined through proton induced X-ray emission (PIXE) measurements and other impurity levels, notably Ca, were below the detection level of around 0.1%. The high level of Nb doping resulted in a low room temperature resistivity of 10^{-3} Ωm which increased with increasing sample temperature. The $SrTiO_3$ crystals were etched for 10 min in a buffered NH_4F–HF solution (BHF) of pH 4.5 according to the recipe published by Kawasaki et al. [16] in order to remove any SrO terminations.

Following the BHF etch the samples were introduced into the UHV chamber of an STM (JEOL JSTM4500XT) operating at a pressure of 10^{-8} Pa. Etched Pt/Ir tips were used to obtain constant current images at room temperature with a bias voltage applied to the sample. LEED was carried out in a 4 mesh VG Microtech rear view system. Sample heating in the UHV chamber was achieved through passing a current through the substrate which allowed anneal temperatures of up to 1400 °C to be reached. Temperature measurement was performed through a viewport with an optical pyrometer.

3. The (1 × 1) reconstruction

BHF etched samples were introduced into the chamber of the STM and heated in UHV for periods of up to 30 min and at temperatures up to 600 °C. These samples showed crisp (1 × 1) LEED patterns. When STM was performed on these samples the images showed a rough surface morphology with no distinct terrace formation. No atomic resolution images could be obtained from these surfaces. Auger electron spectroscopy studies carried out by other researchers [15] on similar samples showed that following a BHF etch there is C contamination present on the surface that requires an anneal temperature of around 570 °C to be removed. It is therefore most likely that in the experiments reported here for the samples where the anneal temperature is below 600 °C the TiO_2 surface layer is covered in at least one monolayer of carbon thereby preventing atomic resolution STM imaging. The (1 × 1) LEED patterns must therefore originate from the ordered $SrTiO_3$ layers beneath the carbon contamination layer.

4. The (2 × 1) reconstruction

On annealing the samples in UHV between 600 and 800 °C for 30 min the carbon contamination is removed [15] and is accompanied by $(1 \times 2) + (2 \times 1)$ spots in the LEED patterns [25]. STM of these samples show terrace formation, and step edges can be seen in the images. For increased anneal temperatures between 800 and 900 °C the surface morphology becomes more regular and gives rise to STM images of the type shown in Fig. 2a where wavy step edges separate 30 nm wide terraces. In all STM images of the (2 × 1) reconstructed surface the step edges do not align themselves with any crystallographic direction. The steps are measured to be around 0.4 nm high as shown in the line scan in Fig. 2b which was taken horizontally through the centre of Fig. 2a. On all (2 × 1) reconstructed surfaces step heights were always 0.4 nm high, which corresponds to the bulk unit cell height of 0.39 nm. No fractional step heights were observed. The terrace structures are therefore crystallographically equivalent with only one type of termination. Therefore, the scenario of mixed TiO_2 and SrO terminations does not apply for the (2 × 1) reconstructed surface in this study.

The atomic structure of the terraces is shown in Fig. 2c where lines separated by around 0.8 nm (equivalent to two bulk unit cells) are seen. LEED patterns reveal a single unit cell periodicity along

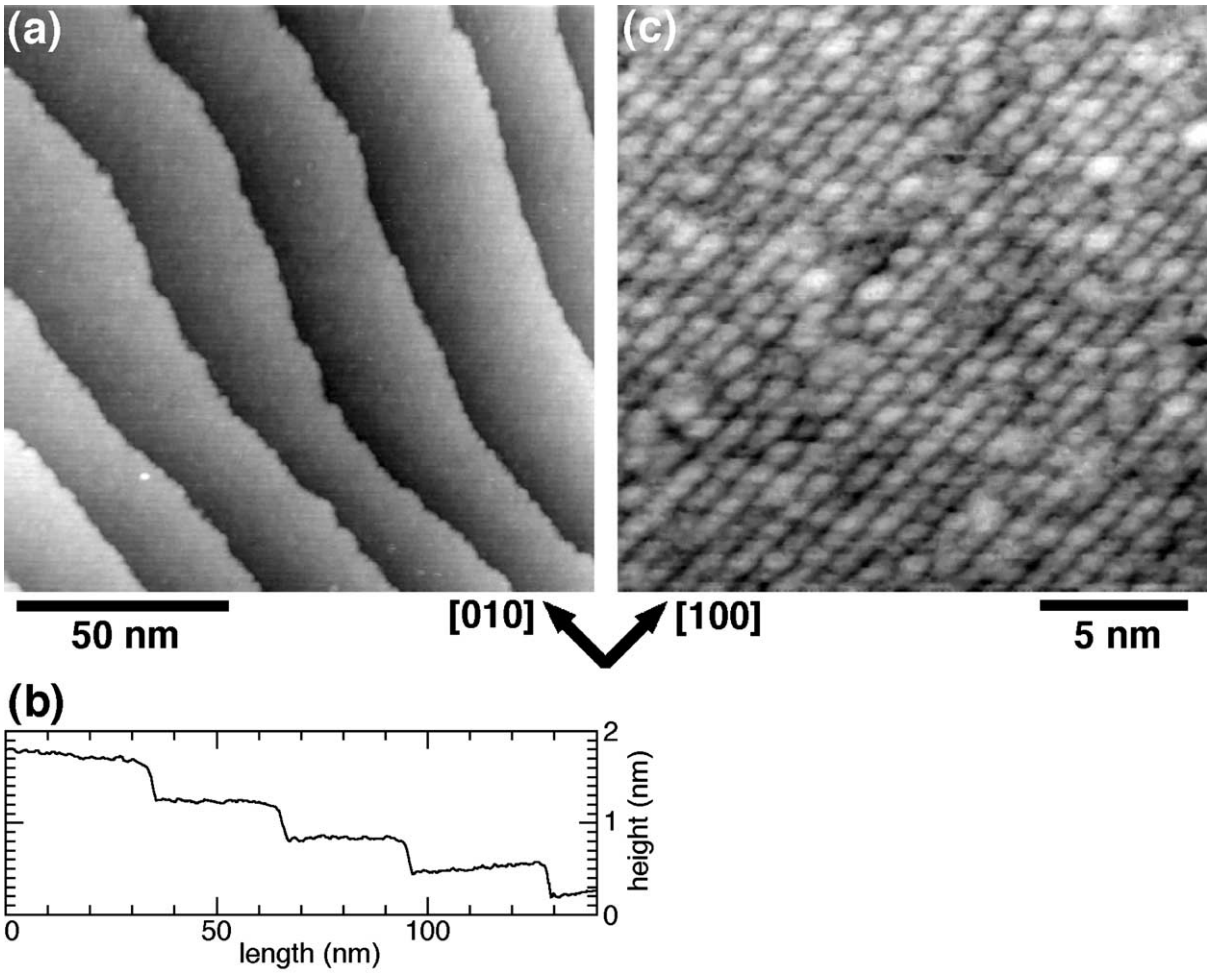

Fig. 2. STM images of the (2 × 1) reconstructed surface. The surface morphology shown in (a) (2.3 V bias, 0.1 nA current) has wavy step edges. A horizontal line scan through the centre of (a) is displayed in (b) showing that the steps are 0.4 nm high which corresponds to one bulk unit cell. A high resolution image of one of the terraces (c) (2.0 V bias, 0.5 nA current) shows the 0.8 nm separation between the lines of the (2 × 1) reconstruction.

the rows, but this cannot be discerned in the STM images. Typical corrugation heights perpendicular to the rows in Fig. 2c are 0.05 nm. LEED patterns show that both the (2 × 1) and (1 × 2) domains are present on the surface. In the present study STM images of different areas of the crystal showed the different domain orientations, i.e. similar images to the one shown in Fig. 2c but rotated through 90° were also obtained. However, no atomic resolution STM images were obtained that showed both domains in the same image. This indicates that the (2 × 1) domains are typically larger than 50 nm which is the maximum scan area where atomic resolution is still maintained. Another report [23] of STM imaging of the (2 × 1) reconstruction on a more defective surface is consistent with the results shown here.

In the STM image in Fig. 2c the bright rows are wider than the gaps between the rows. Furthermore, the typical corrugation height perpendicular to the rows is 0.05 nm indicating that the tip does not have sufficient space between the rows to reach the layer that lies 0.2 nm below. However, when interpreting atomic resolution STM images it can

be very difficult to separate topographic effects from the influence of electronic structure. The topography inversion of empty states STM images of the rutile $TiO_2(1\,1\,0)$ (1×1) surface is a prime example [34]. In future, ab inito calculations of the electronic structure of the (2×1) reconstructed surface of $SrTiO_3(0\,0\,1)$ will need to be performed to help resolve any topography versus electronic structure issues.

During the literature review for this study no reports on ion scattering experiments were found that were specific to the (2×1) surface. However, other ion scattering studies [15,35] on BHF etched and UHV-annealed surfaces indicated that the termination consists of a layer of Ti and O ions. It is therefore reasonable to assume that the (2×1) reconstruction is created through an ordered layer of Ti and O ions that are in epitaxial registry with the Sr and O ions in the SrO layer below. Two models of the atomic structure for the (2×1) surface are proposed here and are shown in Fig. 1. The reconstruction in Fig. 1b has TiO_2 stoichiometry where the surface Ti and O coverage is 50% compared with the (1×1) surface. For the transition from the (1×1) reconstruction to the $TiO_2(2 \times 1)$ reconstruction in Fig. 1b one has to remove every second [0 1 0] row of Ti ions, remove half the O ions, and place the remaining O ions on top of second layer Sr ions. The alternative proposal is shown in Fig. 1c: here the (2×1) reconstruction is created by removing a [0 1 0] row of O ions from the (1×1) surface at two unit cell spacings. The surface stoichiometry then becomes Ti_2O_3.

From a qualitative interpretation alone it is not possible to say which of the (2×1) reconstructions proposed in Fig. 1 better matches the STM images. However, because the TiO_2 termination (Fig. 1b) only has Ti^{4+} ions, and the Ti_2O_3 termination (Fig. 1c) only has Ti^{3+} ions it should be possible to use an electronic structure technique to distinguish between the two surfaces. Indeed, a high concentration of surface states has been detected by ultraviolet photoemission spectroscopy [6,15] and assigned to O surface defects which would therefore give rise to Ti^{3+} species. However, it remains unclear whether the band gap state in the UPS data is due to a (2×1) Ti_2O_3 type termination (Fig. 1c), or random O defects in a TiO_2 type termination such as the (1×1) surface or the (2×1) TiO_2 surface (Fig. 1b).

5. The c(4 × 4) reconstruction

On annealing the (2×1) surface at a temperature of around 900 °C for 30 min LEED patterns start to show a strong central spot and weaker (1/4,1/4) spots indicative of a $c(4 \times 4)$ pattern that is evolving together with the $(2 \times 1) + (1 \times 2)$ pattern. Higher anneal temperatures up to 1400 °C and longer anneal times cause the $c(4 \times 4)$ pattern to increase in intensity. A common feature of the $c(4 \times 4)$ LEED patterns is that the central spot is significantly more intense than the (1/4,1/4) spots. It may therefore be possible to misinterpret a $c(4 \times 4)$ pattern with very weak (1/4,1/4) spots as a (2×2) pattern.

An STM image of a sample annealed in UHV at 1100 °C for 20 min is shown in Fig. 3a. A region of the $c(4 \times 4)$ reconstruction can be seen in the lower terrace, and is surrounded by (2×1) reconstructed areas. The wavy step edge morphology and 0.4 nm step heights remain the same as for the wholly (2×1) reconstructed surface. On annealing these samples in UHV up to 1400 °C for a few minutes both the $c(4 \times 4)$ and (2×1) reconstructions were still visible within a 50×50 nm STM scan area. This indicates that both reconstructions can coexist up to high anneal temperatures.

A high resolution image of the $c(4 \times 4)$ reconstruction is shown in Fig. 3b where the $c(4 \times 4)$ surface unit cell has been drawn into the figure. A small region towards the centre of the image is still (2×1) reconstructed. The $c(4 \times 4)$ reconstruction appears to consist of lines that run in the [1 0 0] direction and have a break every 1.6 nm (four bulk unit cells). The breaks in the neighbouring lines are offset which produces a ''brickwork'' pattern. The $c(4 \times 4)$ reconstruction appears to evolve from the (2×1) areas through ordering of defects. This means that the $c(4 \times 4)$ brickwork pattern can have two domains where the units can run along either the [1 0 0] or [0 1 0] directions. Both domain types were seen in STM images.

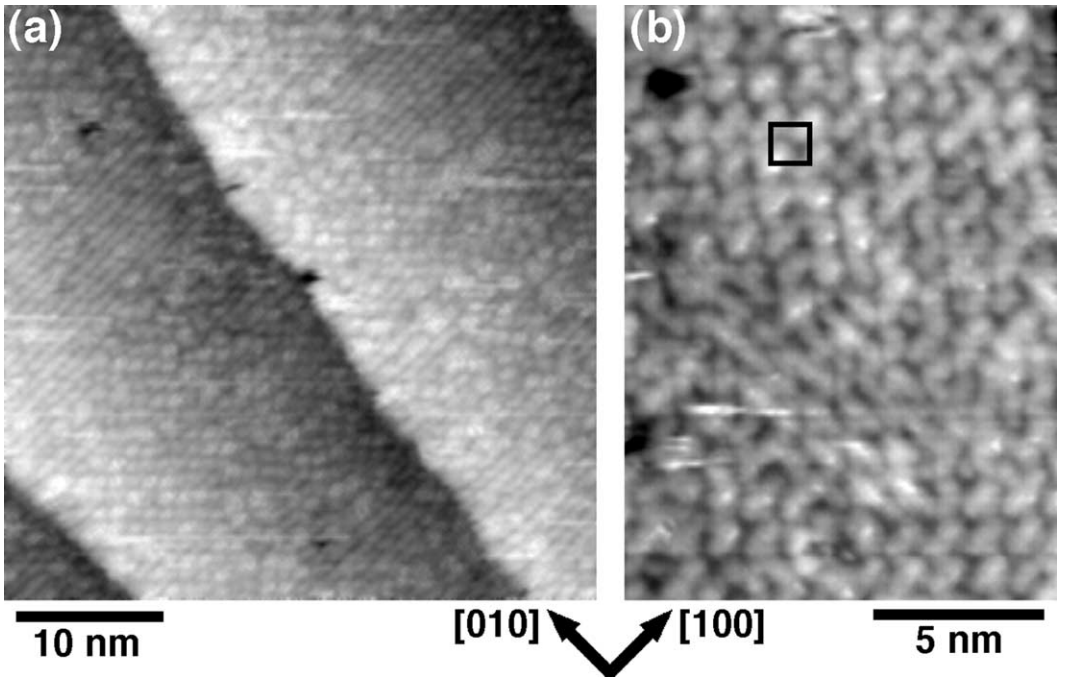

Fig. 3. STM images of the $(2 \times 1) + c(4 \times 4)$ reconstructed surface. In (a) (2.0 V bias, 0.1 nA current) a region of $c(4 \times 4)$ on the lower terrace is surrounded by (2×1) reconstructed areas. The step height between terraces is 0.4 nm. In (b) (0.2 V bias, 10 nA current) the surface is mainly $c(4 \times 4)$ reconstructed and the $c(4 \times 4)$ unit cell is shown.

Two proposed models of the $c(4 \times 4)$ reconstruction are shown in Fig. 4 which have evolved from the two proposed (2×1) terminations of Fig. 1. The $c(4 \times 4)$ reconstruction of Fig. 4a can be created by removing every fourth TiO_2 unit along the lines of the (2×1) reconstruction of Fig. 1b. This results in a $c(4 \times 4)$ reconstruction with TiO_2 stoichiometry. The alternative proposal shown in Fig. 4b is created by removal of every fourth pair of O ions from the rows in the (2×1) reconstruction of Fig. 1c. This gives rise to a $c(4 \times 4)$ reconstruction with Ti_4O_5 stoichiometry.

As with the (2×1) surface, it is not possible to distinguish between the alternative $c(4 \times 4)$ models using only STM image data. But again, probes of the electronic surface structure would help to distinguish the proposed models. In the TiO_2 termination (Fig. 4a) only Ti^{4+} ions are present, whereas in the Ti_4O_5 termination (Fig. 4b) only Ti^{3+} and Ti^{2+} ions appear. However, as the work here is the first report of the $c(4 \times 4)$ reconstruction it is not possible to draw on previously published data.

6. The $c(4 \times 2)$ reconstruction

The creation of the (2×1) and $c(4 \times 4)$ reconstructions reported above was achieved through BHF etching and UHV annealing only. However, an alternative $c(4 \times 2)$ reconstruction is found when argon ion sputtering is used. Fig. 5a shows the morphology of a $SrTiO_3(0\,0\,1)$ surface following argon ion sputtering (10 min, 500 eV energy, 7 μA current) and UHV annealing at 1200 °C for 15 min which gives rise to a $c(4 \times 2)$ pattern in LEED. Similar STM images can be obtained from samples that have been sputtered and annealed at temperatures in the range 900–1400 °C. Annealing in the 900–1150 °C range also leads to the formation of distinct one dimensional nanostructures that will form the topic of a separate paper [11]. The step heights in Fig. 5a are 0.4 nm (one bulk unit cell) indicating that the surface has only one type of termination. The step edges are straight and aligned with the [0 1 0] and [1 0 0] crystallographic directions.

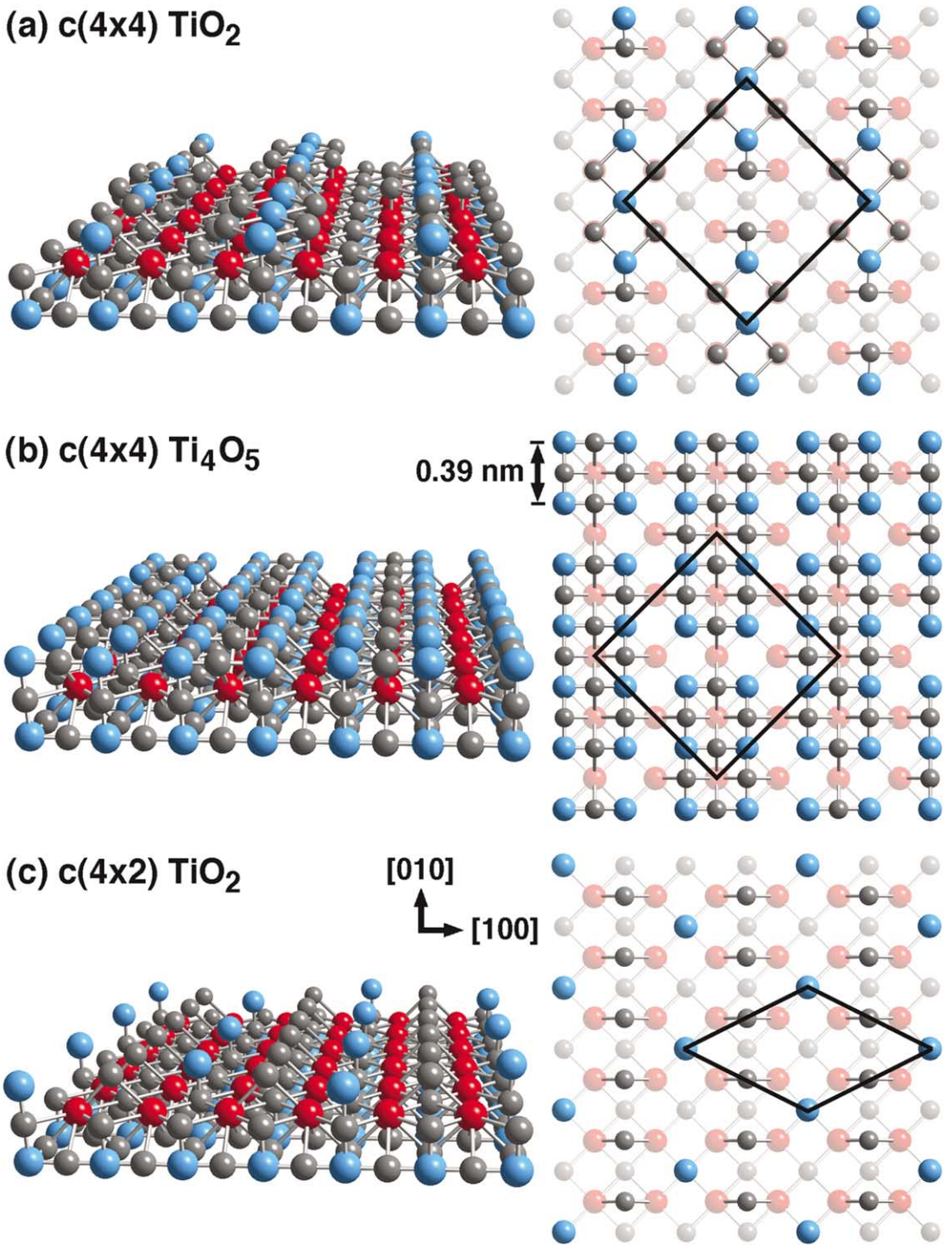
(a) c(4x4) TiO2
(b) c(4x4) Ti4O5
0.39 nm
(c) c(4x2) TiO2
[010]
[100]

Fig. 4. (a) Proposed structure of the c(4 × 4) reconstructed surface with TiO_2 stoichiometry. (b) Proposed structure of the c(4 × 4) reconstructed surface with Ti_4O_5 stoichiometry. (c) Proposed structure of the c(4 × 2) reconstructed surface with TiO_2 stoichiometry. Ti (blue) and O (grey) ions terminate the structures shown in oblique view (left panels) and top view (right panels). In the top view models the unit cells are shown and the underlying SrO layer (Sr in red) is indicated with reduced depth of colour.

An atomic resolution STM image of one of the terraces is shown in Fig. 5b. Both c(4 × 2) domains are visible in the same image and their unit cells are indicated in the figure. The LEED pattern obtained from this two domain c(4 × 2) reconstructed surface is similar to that observed by Andersen and Møller [13] and Jiang and Zegenhagen [25]. Previously reported STM images [25] of the c(4 × 2) reconstruction are consistent with Fig. 5. The surface is still assumed to be Ti and O terminated although the sputtering process will have exposed both SrO and TiO_2 terminations to the vacuum. It cannot be stated with certainty that the c(4 × 2) reconstructed surface is a Ti and O terminated surface until ion scattering experiments have been carried out, but it is certain that only one type of termination exists because the steps are one unit cell high. It is more likely to be the Ti and O termination because this is the surface that existed prior to sputtering, and if the c(4 × 2) reconstruction were Sr and O terminated then following a short sputter and anneal one would expect to see a two termination surface, but that is not observed.

Atomic resolution STM imaging can often be complicated by anomalous tip–surface interactions. A good example of this is the species dependence of the tip apex atom that results in a contrast inversion of O atoms adsorbed on the Ni(1 1 0) or Cu(1 1 0) surfaces [36]. A similar effect

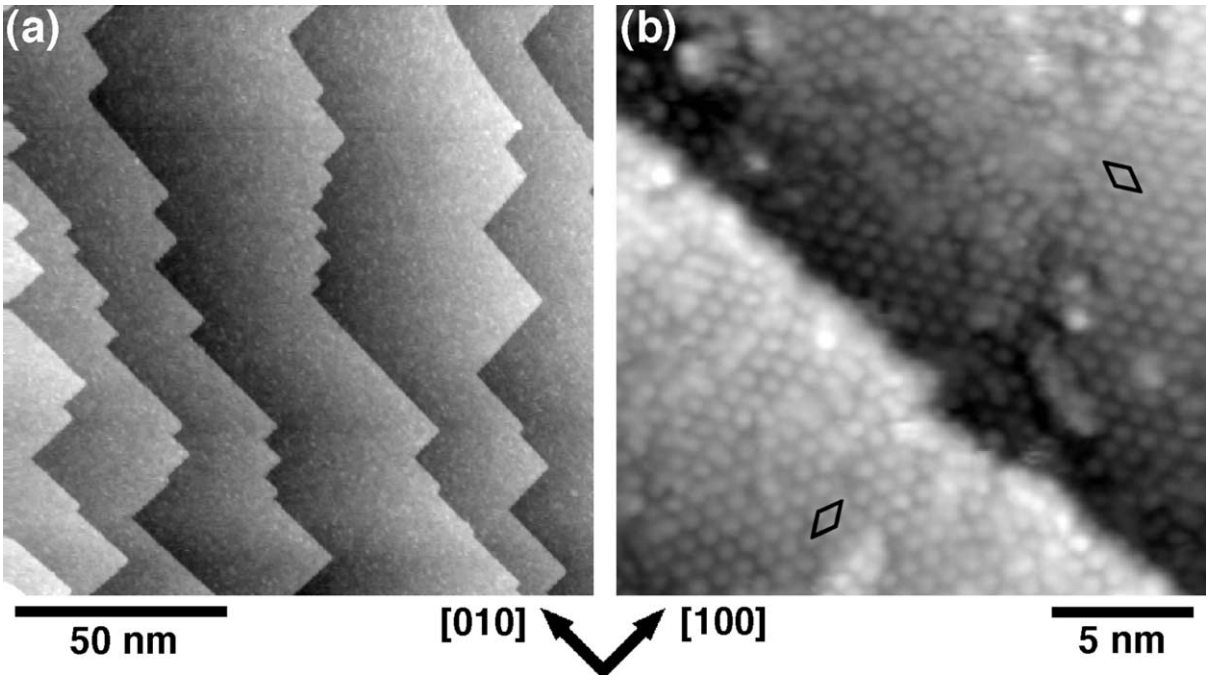

Fig. 5. STM images of the c(4 × 2) reconstructed surface. The surface morphology shown in (a) (2.5 V bias, 0.2 nA current) has straight step edges that follow [0 1 0] and [1 0 0] directions. The step height between terraces is 0.4 nm. An atomic resolution image of one of the terraces (b) (2.0 V bias, 0.1 nA current) shows the two domains of the c(4 × 2) reconstruction indicated by unit cells.

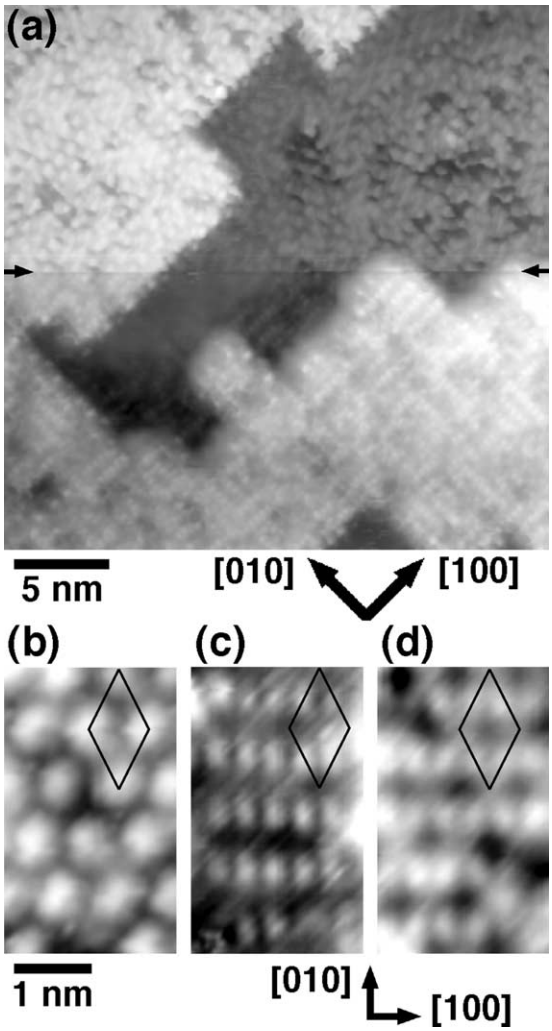

Fig. 6. STM images of the c(4 × 2) reconstructed surface. In (a) (0.87 V bias, 0.15 nA current) the top of the image contains one spot per c(4 × 2) unit cell similar to the image from another region shown in (b) (2.0 V bias, 0.1 nA current). Following a tip change indicated by arrows (but no other change in instrument parameters) half way through the image in (a) two spots per unit cell are seen. This is also observed in other regions as shown in (c) (0.25 V bias, 1 nA current). Sometimes a hybrid of the two images in (b) and (c) is observed as shown in (d) (0.45 V bias, 0.44 nA current). The c(2 × 4) unit cells are indicated in (b–d). Note that the crystallographic directions in (a) are rotated by 45° relative to (b–d).

is reported here for the $SrTiO_3(0\,0\,1)c(4 \times 2)$ reconstruction. In Fig. 6a the slow scan direction is from the top to the bottom of the image. Half way through taking the image (indicated by arrows), and without changing any imaging conditions, a tip change occurs and the atomic contrast changes dramatically. In the top part of Fig. 6a there is one spot per c(4 × 2) surface unit cell, whereas in the bottom part of the image there are two spots per c(4 × 2) surface unit cell. A close up of a region from a different part of the sample taken under different imaging condition with one spot per unit cell is shown in Fig. 6b. The panel next to it (Fig. 6c) shows an image with two spots per unit cell, while Fig. 6d shows an image where both types of unit cell are seen in the same image. It is important to stress that whether one or two spots per unit cell are seen does not depend on imaging conditions like bias voltage or tunnelling current, but instead apparently on the atomic species of the tip apex atom.

The significant difference in atomic surface structure that is seen when comparing Fig. 6b and c suggests that the change in tip apex atom allows different surface sub-lattices to be observed. As the sample surface is still assumed to be Ti and O terminated, a reasonable STM image interpretation is that Fig. 6b shows the Ti surface lattice and that Fig. 6c shows the O surface lattice. Fig. 6d combines imaging of both sub-lattices. The question that immediately arises with this image interpretation is: why are not two sub-lattices observed in the (2 × 1) and c(4 × 4) reconstructions? The answer may be that in fact the two sub-lattices are seen, but that in the case of the (2 × 1) and c(4 × 4) reconstructions detecting the O and Ti ion sub-lattices does not give rise to strikingly different STM images.

A proposed model of the c(4 × 2) reconstructed surface based on qualitative interpretation of the STM images in Figs. 5 and 6 is shown in Fig. 4c with the c(4 × 2) unit cell indicated. The surface layer contains twice as many O as Ti ions and is therefore of TiO_2 stoichiometry. The density of coverage of the TiO_2 c(4 × 2) reconstructed surface is only 25% of the $TiO_2(1 \times 1)$ terminated surface. Furthermore, the surface O^{2-} ions and the surface Ti^{4+} ions are 0.44 nm apart, compared to 0.2 nm in the bulk. This means that the bonding between these ions is weak compared with the bonding to the SrO lattice

below. Henrich et al. [6] used UPS to detect two different band gap states, one of which was only seen in samples that had been argon ion sputtered and annealed. It is possible that this sputtering related band gap state is produced by the type of surface coverage that results in the c(4 × 2) reconstructed surface.

7. Discussion and conclusion

The interpretation of the STM images in the previous sections takes no account of the high Nb doping (0.5% molar) of the crystals, although some of the properties of Nb-doped $SrTiO_3$ are very different compared with undoped stoichiometric $SrTiO_3$. However, these differences are mainly to do with electronic structure rather than surface crystal structure. The (2 × 1) and c(4 × 2) reconstructions have also been observed on pure $SrTiO_3$ crystals that were annealed in UHV and made semiconducting through generation of oxygen vacancies [25]. I have also observed these reconstructions on La-doped crystals. Therefore, the (2 × 1), c(4 × 4) and c(4 × 2) reconstructions are not formed through Nb segregation to the surface. Furthermore, no reports of surface Nb segregation could be found in the literature, and Nb in known not to segregate to grain boundaries in Nb-doped $SrTiO_3$ polycrystals [37].

A striking feature of the terrace images of the (2 × 1) (Fig. 2a) and c(4 × 2) (Fig. 5a) reconstructed surfaces is the nature of the step edges. In the anneal temperature range 800–1400 °C the (2 × 1) surfaces always have wavy step edges and the c(4 × 2) surfaces always have straight step edges aligned with the ⟨1 0 0⟩ directions. The anneal temperatures are high enough to allow the step edges to be dynamic, so it is most likely that the kink formation energy is low on the (2 × 1) surfaces thereby giving rise to wavy step edges. In contrast the kink energy must be high for the c(4 × 2) surfaces, causing straight step edges.

In summary, atomic resolution STM images of the (2 × 1), c(4 × 4), and c(4 × 2) reconstructions on Nb-doped $SrTiO_3$(0 0 1) surfaces have been shown. The (2 × 1) and c(4 × 4) surfaces were created through annealing a BHF etched sample in UHV, and the c(4 × 2) surface was created through Ar^+ ion sputtering and then annealing in UHV. Only unit cell step heights and no two termination effects (simultaneous TiO_2 and SrO terminations) were observed on any of the reconstructed surfaces. The nature of the step edges is quite different for the reconstructions: the (2 × 1) and c(4 × 4) surfaces have a low energy for kink formation, but the c(4 × 2) surface has a relatively high energy. When imaging the c(4 × 2) surface the nature of the tip apex atom is responsible for revealing either the Ti or the O surface sub-lattices. Surface atomic structure models are proposed for the reconstructions. Cases are presented for Ti and O terminated surfaces with partially covered TiO_2 terminations, or alternatively with Ti_2O_3 or Ti_4O_5 stoichiometry.

To further investigate the reconstructions on $SrTiO_3$(0 0 1) surfaces and to test the proposed atomic structure models it will be necessary to go beyond electron diffraction and STM. The next step is to use a highly surface sensitive chemical and structural technique such as coaxial impact collision ion scattering spectroscopy (CAICISS) in conjunction with ab initio modelling. These studies are currently underway and should be able to resolve the detailed atomic structure of the $SrTiO_3$(0 0 1) reconstructions.

Acknowledgements

I would like to thank the Royal Society for funding, and Thomas Wagner, Peter Hoffmann, Bryan Huey, Karin Rabe, Andrew Briggs, Tony Paxton, Karen Johnston, Mike Finnis and John Pethica for stimulating discussions.

References

[1] R.A. McKee, F.J. Walker, M.F. Chisholm, Crystalline oxides on silicon: the first five monolayers, Phys. Rev. Lett. 81 (1998) 3014–3017.
[2] R.A. McKee, F.J. Walker, M.F. Chisholm, Physical structure and inversion charge at a semiconductor interface with a crystalline oxide, Science 293 (2001) 468–471.
[3] K. Pennicott, GaAs meets its match, Phys. World 14 (2001) 6.

[4] B. Meyer, J. Padilla, D. Vanderbilt, Theory of $PbTiO_3$, $BaTiO_3$, and $SrTiO_3$ surfaces, Faraday Discuss. (1999) 395–405.
[5] J. Padilla, D. Vanderbilt, Ab initio study of $SrTiO_3$ surfaces, Surf. Sci. 418 (1998) 64–70.
[6] V.E. Henrich, G. Dresselhaus, H.J. Zeiger, Surface defects and the electronic structure of $SrTiO_3$ surfaces, Phys. Rev. B 17 (1978) 4908–4921.
[7] B. Reihl, J.G. Bednorz, K.A. Muller, Y. Jugnet, G. Landgren, J.F. Morar, Electronic-structure of strontium-titanate, Phys. Rev. B 30 (1984) 803–806.
[8] P.J. Moller, S.A. Komolov, E.F. Lazneva, A total current spectroscopy study of metal oxide surfaces: II. Unoccupied electronic states on $TiO_2(110)$ and $SrTiO_3(100)$ surfaces, J. Phys.-Condes. Matter 12 (2000) 7705–7711.
[9] K. van Benthem, R.H. French, W. Sigle, C. Elsasser, M. Ruhle, Valence electron energy loss study of Fe-doped $SrTiO_3$ and a Sigma 13 boundary: electronic structure and dispersion forces, Ultramicroscopy 86 (2001) 303–318.
[10] T. Higuchi, T. Tsukamoto, N. Sata, M. Ishigame, Y. Tezuka, S. Shin, Electronic structure of p-type $SrTiO_3$ by photoemission spectroscopy, Phys. Rev. B 57 (1998) 6978–6983.
[11] M.R. Castell, Nanostructures on the $SrTiO_3(001)$ surface studied by STM, in preparation.
[12] A. Ikeda, T. Nishimura, T. Morishita, Y. Kido, Surface relaxation and rumpling of TiO_2-terminated $SrTiO_3(001)$ determined by medium energy ion scattering, Surf. Sci. 435 (1999) 520–524.
[13] J.E.T. Andersen, P.J. Moller, Impurity-Induced 900-Degrees-C (2×2) surface reconstruction of $SrTiO_3(100)$, Appl. Phys. Lett. 56 (1990) 1847–1849.
[14] G. Charlton, S. Brennan, C.A. Muryn, R. McGrath, D. Norman, T.S. Turner, G. Thornton, Surface relaxation of $SrTiO_3(001)$, Surf. Sci. 457 (2000) L376–L380.
[15] T. Nishimura, A. Ikeda, H. Namba, T. Morishita, Y. Kido, Structure change of TiO_2-terminated $SrTiO_3(001)$ surfaces by annealing in O-2 atmosphere and ultrahigh vacuum, Surf. Sci. 421 (1999) 273–278.
[16] M. Kawasaki, K. Takahashi, T. Maeda, R. Tsuchiya, M. Shinohara, O. Ishiyama, T. Yonezawa, M. Yoshimoto, H. Koinuma, Atomic control of the $SrTiO_3$ crystal-surface, Science 266 (1994) 1540–1542.
[17] T. Nakamura, H. Inada, M. Iiyama, In situ surface characterization of $SrTiO_3(100)$ substrates and homoepitaxial $SrTiO_3$ thin films grown by molecular beam epitaxy and pulsed laser deposition, Appl. Surf. Sci. 132 (1998) 576–581.
[18] M. Lippmaa, M. Kawasaki, A. Ohtomo, T. Sato, M. Iwatsuki, H. Koinuma, Observation of $SrTiO_3$ step edge dynamics by real-time high-temperature STM, Appl. Surf. Sci. 132 (1998) 582–586.
[19] H. Tanaka, T. Matsumoto, T. Kawai, S. Kawai, Surface-structure and electronic property of reduced $SrTiO_3(100)$ surface observed by scanning tunneling microscopy spectroscopy, Jpn. J. Appl. Phys. Part 1—Regul. Pap. Short Notes Rev. Pap. 32 (1993) 1405–1409.
[20] Y. Liang, D.A. Bonnell, Structures and chemistry of the annealed $SrTiO_3(001)$ surface, Surf. Sci. 310 (1994) 128–134.
[21] A.D. Polli, T. Wagner, M. Ruhle, Effect of Ca impurities and wet chemical etching on the surface morphology of $SrTiO_3$ substrates, Surf. Sci. 429 (1999) 237–245.
[22] J. Zegenhagen, T. Haage, Q.D. Jiang, Microscopic structure and structuring of perovskite surfaces and interfaces: $SrTiO_3$, $RBa_2Cu_3O_{3-\delta}$, Appl. Phys. A-Mater. Sci. Process. 67 (1998) 711–722.
[23] Q.D. Jiang, J. Zegenhagen, $SrTiO_3(001)$ surfaces and growth of ultra-thin $GdBa_2Cu_3O_{7-x}$ films studied by LEED/AES and UHV-STM, Surf. Sci. 338 (1995) L882–L888.
[24] Q.D. Jiang, J. Zegenhagen, $SrTiO_3(001)$-c(6×2): a long-range, atomically ordered surface stable in oxygen and ambient air, Surf. Sci. 367 (1996) L42–L46.
[25] Q.D. Jiang, J. Zegenhagen, c(6×2) and c(4×2)-reconstruction of $SrTiO_3(001)$, Surf. Sci. 425 (1999) 343–354.
[26] K. Iwahori, S. Watanabe, M. Kawai, K. Mizuno, K. Sasaki, M. Yoshimoto, Nanoscale composition analysis of atomically flat $SrTiO_3(001)$ by friction force microscopy, J. Appl. Phys. 88 (2000) 7099–7103.
[27] J. Fompeyrine, R. Berger, H.P. Lang, J. Perret, E. Machler, C. Gerber, J.P. Locquet, Local determination of the stacking sequence of layered materials, Appl. Phys. Lett. 72 (1998) 1697–1699.
[28] P.J. Moller, S.A. Komolov, E.F. Lazneva, Selective growth of a $MgO(100)$-c(2×2) superstructure on a $SrTiO_3(100)$-(2×2) substrate, Surf. Sci. 425 (1999) 15–21.
[29] M. Naito, H. Sato, Reflection high-energy electron-diffraction study on the $SrTiO_3$ surface-structure, Physica C 229 (1994) 1–11.
[30] T. Matsumoto, H. Tanaka, T. Kawai, S. Kawai, STM-imaging of a $SrTiO_3(100)$ surface with atomic-scale resolution, Surf. Sci. 278 (1992) L153–L158.
[31] T. Matsumoto, H. Tanaka, K. Kouguchi, T. Kawai, S. Kawai, A scanning-tunneling-microscopy study of laser molecular-beam epitaxy on $SrTiO_3(100)$ surface, Surf. Sci. 312 (1994) 21–30.
[32] H. Tanaka, T. Matsumoto, T. Kawai, S. Kawai, Interaction of oxygen vacancies with O-2 on a reduced $SrTiO_3(100)(\sqrt{5} \times \sqrt{5})R26.6°$ surface observed by STM, Surf. Sci. 318 (1994) 29–38.
[33] T. Kubo, H. Nozoye, Surface structure of $SrTiO_3(100)$-$(\sqrt{5} \times \sqrt{5})R26.6°$, Phys. Rev. Lett. 86 (2001) 1801–1804.
[34] Q.D. Jiang, J. Zegenhagen, $SrTiO_3(001)$-c(6×2): a long-range, atomically ordered surface stable in oxygen and ambient air, Surf. Sci. 367 (1996) L42–L46.
[35] P.A.W. van der Heide, Q.D. Jiang, Y.S. Kim, J.W. Rabalais, X-ray photoelectron spectroscopic and ion

scattering study of the $SrTiO_3(001)$ surface, Surf. Sci. 473 (2001) 59–70.

[36] L. Ruan, F. Besenbacher, I. Stensgaard, E. Laegsgaard, Atom-resolved discrimination of chemically different elements on metal-surfaces, Phys. Rev. Lett. 70 (1993) 4079–4082.

[37] Z.G. Mao, R.E. Dunin-Borkowski, C.B. Boothroyd, K.M. Knowles, Direct measurement and interpretation of electrostatic potentials at 24 degrees [001] tilt boundaries in undoped and niobium-doped strontium titanate bicrystals, J. Am. Ceram. Soc. 81 (1998) 2917–2926.